The Hydro-Thermal Influence of Fault Attributes on the Geothermal Reservoir Behaviour

By

Y.M. van Hout

Bachelor Thesis

Delft University of Technology
Faculty of Civil Engineering and Geosciences
Bachelor Applied Earth Sciences

To be defended publicly on Wednesday January 24th, 2018 at 10:00 AM

Supervisors: Dr. N. Golizadeh Doonechaly, Petroleum Engineering TU Delft
Prof. Dr. G. Bertotti TU Delft, Applied Geology TU Delft

Thesis committee: Prof. Dr. G. Bertotti TU Delft, Applied Geology TU Delft
Dr. ir. A.A.M. Dieudonne, Geo-Engineering TU Delft

Abstract

The fluid flow in a reservoir largely depends on faults, as faults can act like conduits or barriers. The influence of three fault parameters (permeability, thickness and angle) on the temperature and pressure behaviour of a geothermal reservoir, has been investigated by modelling a faulted reservoir in 2D in MATLAB, based on the Finite Element Method.

The reservoir is assumed to be sandstone with a permeability of $40*10^{-14}$ m^2. The fault has been modelled with a permeability ranging from 10^{-11} m^2 to 10^{-17} m^2, a thickness ranging from 10 cm to 150 m and an angle ranging from 0 to 90 degrees. While varying one parameter, the other two stayed fixed. The base values for the fault permeability, thickness and angle were 10^{-14} m^2, 20 m and 0 degrees respectively. Both a finite and infinite fault have been modelled in the reservoir.

Decreasing the permeability led to a higher production temperature, especially at a finite fault, where the fluid is able to bypass the fault and thus sweep the warmth of a larger part of the reservoir. At a fault permeability of 10^{-14} m^2 the fluid has seemed to have extracted the maximum amount of heat in the reservoir, further decrease in permeability did not lead to a higher production temperature. At an infinite fault there is only a small increase in temperature at a fault permeability of 10^{-16} m^2. The impedance at a finite fault is not much affected, as the fluid is able to flow around the fault. The impedance at an infinite fault, however, rapidly builds up with decreasing permeability.

A thickness of 20 m, at the base permeability value of 10^{-14} m^2, results in the highest production temperature. Larger thicknesses cause larger amounts of unrecoverable area and consequently less heat can be extracted. At a finite fault the impedance climbs only to a value of 4 MPa at a thickness of 150 m, but at an infinite fault the impedance already reaches 10 MPa at a thickness of 80 m.

The fault has its largest influence at a perpendicular position to the flow. At a parallel position, the results are the same as a reservoir without fault, as the fluid will not have to dodge a lot to reach the production well.

All three fault parameters have a significant influence on the temperature and pressure behaviour of the geothermal reservoir. They are all able to enlarge and eliminate the influence of the fault. A finite fault can cause a favourable higher production temperature without a large impedance, as the fluid is able to bypass the fault. An infinite fault has less effect on the temperature and causes the impedance to build up rapidly, which requires an unrealistic high pumping power and consequently an unprofitable geothermal system.

Contents

Introduction

Nowadays there is an increasing interest in developing geothermal projects, as it is a sustainable energy source. Over the years, the Netherlands have mostly been developing geothermal doublet systems in order to warm up greenhouses and houses. For electricity generation, a high thermal gradient is required, which is not yet the case in the subsurface of the Netherlands. Because of the lower thermal gradient, the feasibility of geothermal projects might still be questionable. In addition, geothermal wells require large investment costs and mainly the fact that the subsurface has large uncertainties slows down the development (C. Willems, 2017). The expected lifetime of a geothermal system is one of the most important aspects of determining whether developing a system is profitable or not (R.C.A. Smit, 2012). The lifetime depends on various reservoir properties: temperature, pressure, permeability distribution, flow rate and doublet spacing, among others. The geothermal reservoir is mainly influenced by the subsurface fluid flow, which is highly dependent of fault zone permeability (Moeck, 2014). Faults can be pathways or obstacles for fluid flow and can significantly affect the flow, and thus the performance, of the reservoir. Therefore, to estimate the profitability of the project, it is important to be able to predict the influence of a fault on a reservoir.

In this thesis, the influence of fault parameters on geothermal reservoir performance will be investigated in a hydro-thermal framework. The performance of the reservoir will be measured on the basis of the temperature and pressure behaviour of the reservoir. This will be investigated by using a MATLAB model for the fluid flow and heat transfer, which are the two main physical processes in a reservoir. The model is 2D and based on the finite element method. In this research, both a finite and infinite fault will be simulated in the model with three varying parameters: permeability, thickness and angle.

First geothermal reservoir and fault properties that were important for the modelling are discussed, followed by a description of the method in MATLAB. Next, the experiment sets and results are discussed and in the final chapters the conclusion, discussion and recommendations are stated.

1. Geothermal Reservoir Properties

In the following paragraphs, a few aspects and parameters of geothermal doublet systems are described that were important for the modelling.

1.1. Reservoir Temperature and Permeability

A geothermal reservoir consists of highly permeable rock. This is essential as the reservoir must be able to contain lots of water and the pores should be interconnected for the water to flow from the injection well to the production well. Usually geothermal reservoirs are found in fractured volcanic rocks, such as in Iceland. The fluid is then found in the fractures, not in the pores, and the thermal gradient in such areas can reach 200 degrees per kilometre (A. Hjartarson, 2015). In the Netherlands, most of the geothermal doublets have been developed in the West Netherlands Basin (WNB). The reservoir is the fluvial Delft Sandstone Member which is part of the Cretaceous Nieuwekerk formation (Van Adrichem Boogaert and Kouwe, 1993) and the thermal gradient in the Netherlands is about 30 degrees per kilometre (D. Bonté, J.D. van Wees & J.M. Verweij, 2012). In the Delft Sandstone Member reservoir, the depth ranges from 2 to 3 km and the temperature of the aquifer ranges from 70 to 90 degrees (C.J.L. Willems, 2017). Currently a new well is being drilled in the Netherlands, the Trias Westland Project. On 'nlog' the properties of this well (LIR-45) are listed and this well goes to a depth of approximately 3 to 4 kilometres. The well reaches the 'Hardegsen Formation' until the 'Lower Volpriehausen Sandstone Member'. These layers are part of the Main Buntsandstein which is a subgroup of the Triassic. To link some values of this thesis to a realistic case, this 'Trias Westland Project' has been taken as reference project. The permeability of the Buntsandstein is relatively low, however, this can be increased by hydraulic stimulation. Therefore, the permeability value of the reservoir taken in the model is $40*10^{-14}$ m^2, a bit higher than the general value of Fresh Sandstone, 10^{-14} m^2 (Bear, 1972). A reservoir temperature of 140 degrees is expected at the Trias Westland Project, which will also be the value of the reservoir temperature in this thesis.

A geothermal reservoir is naturally in dynamic condition, it is in a continuous state of convective flow, with a constant heat supply coming from all four sides of the reservoir. The heat supply will be more or less constant during the whole research so it will not significantly affect the modelling, since it is a comparison study of different fault scenarios and not a calculation of the total recoverable energy for example.

1.2. Reservoir Pressure

The production and injection of water in a geothermal reservoir result in a pressure difference, which results into fluid flow (B. Steingrimsson, 2013). At the injection well, the pressure rises and at the production well, the pressure decreases, which drives the flow from the injection well to the production well. A steady flow with a small impedance is desired, as a large impedance requires a higher pumping power. Just a little amount of overpressure would be the best-case scenario. At an impedance larger than 10 MPa it is usually not worth it to produce from that reservoir. The lower the permeability of the reservoir, the higher the impedance will be. This can be described at the basis of Darcy's equation for fluid flow. The pressure of the water in the reservoir during initial conditions in the model is 34 MPa, this corresponds to a depth of 3.4 kilometres as the water pressure follows a hydrostatic profile. The reservoir then has a static pressure that is unaffected and completely depends on the reservoir fluid density. During injection, the well has a different pressure than the reservoir, which results in a high-pressure gradient at the near well area.

1.3. Well Spacing

The well spacing of the geothermal doublets in the West Netherlands Basin is between 1 and 1.5 km. (C.J.L. Willems *et al.*, 2017) In this thesis the well distance is 400 metres. This is due to the running time of the MATLAB script and the Random-Access Memory of the computer. For an easier and quicker computation, a small reservoir and well spacing have been chosen. The whole reservoir has a size of 600 m x 300 m.

1.4. Fluids in the Well and Reservoir

The fluid in the reservoir can be gas or liquid, and it can be meteoric, sea water or magmatic (K. Nicholson, 1993). The fluids in the well and reservoir are water. The initial pressure of the reservoir is assumed to be 34 MPa, which is equal to 340 Atm, which is high enough for the water to be in the liquid phase at a temperature of 140 degrees (see Figure 1). The boiling and gas phase are not considered in the model since the reservoir is assumed to be in single phase.

The injection water has a temperature of 40 degrees, this is also the approximate injection temperature in the Netherlands (C.J.L. Willems *et al.,* 2017). A typical enhanced geothermal system has a flow rate of 100 L/s for the whole reservoir. The thickness of the reservoir could vary a lot, a possible thickness of 100 m has been chosen in this thesis. As the model in this thesis is 2D, the value of 100 L/s has to be divided by its thickness. Thus, the flow rate now becomes 1 L/s, which is 0.001 m^3/s. The flow rate will be fixed everywhere in the reservoir for every time step.

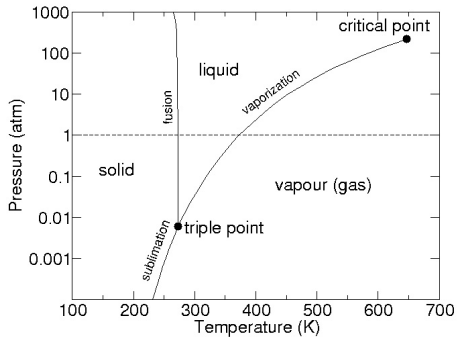

Figure 1: Phase diagram of water

1.5. Well Radius

After well stimulation, the effective well radius becomes larger than the actual well radius. Well stimulation treatments improve the permeability of the near-well formation and thus the well productivity. In sandstones for example, the formation damage is removed by dissolving the material that is plugging the pores or by increasing the pore spaces. The treatment fluid is usually acid (R.C.M. Malate & J.J.C. Austria, 1998). The actual radius of the injection well is 21.60 cm (M.Z. Lukawski, *et al*., 2014), while the effective well radius used in this thesis has the value of 1 m.

2. Fault Properties

As written in the introduction, faults influence the flow in a reservoir. The fault zone usually consists of a fault core and a damage zone, as seen in Figure 2 (Cowie & Sholz, 1992). They do not both have to be present. In the fault core, most of the displacement has taken place. It can be a single slip surface, clay rich gouge zone, brecciated, chemically effected or cataclasite zone. Damage zones consist of deformation bands, veins, fractures, cleavage and faults. The permeability of the fault mainly depends on the grains of the fault rock in the core and on the fracture network of the damage zone (J.S. Caine, J.P. Evans & C.B. Forster, 1996). In porous sandstones three different faults can form: slip surfaces, single deformation bands and zones of deformation bands (Aydin & John-son, 1978). Deformation bands are small faults with small displacements consisting of small grains, poor sorting and thus lower porosity (R. Schultz, 2009). Because of the different permeability values the fault can have compared to the host rock, it can behave like a barrier, or the opposite, a pathway. If faults act like a barrier, they can trap the water, which can even lead to over pressuring (E.C.D. Hooper, 1991). In this thesis, the model has been tested with a varying fault permeability, fault thickness and fault angle with the faults' location in the middle of the reservoir.

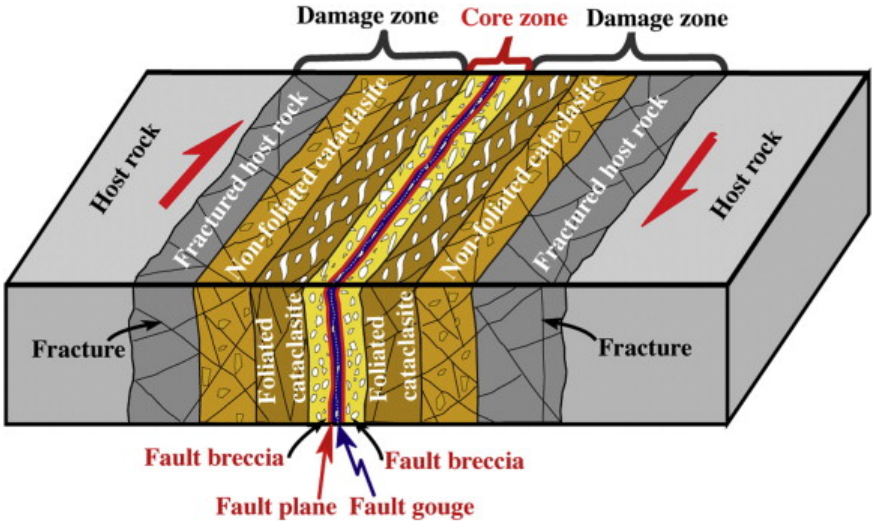

Figure 2: Schematic model of a fault core zone and damage zone within a strike-slip fault zone (Cowie & Scholz, 1992)

2.1. Permeability

The permeability of the fault depends on the amount of cataclasis, clay content, autogenic minerals and diagenetic precipitation of cement (M. Antonellini & A. Aydin, 1994). Due to shearing of a sandstone rock, the grainsize decreases in the fault core. This results into clay that will significantly decrease the permeability of the fault zone, and will thus result into a barrier for the flow perpendicular to the fault. However, the damage zone can also contain higher permeability areas due to fractures and breccia, such as along the slip plane discontinuity, and this will result into flow parallel to the fault (G. C. Rawling, L.B. Goodwin & J.L. Wilson 2001). In Figure 3, three possible situations of a normalized permeability along a fault zone are displayed.

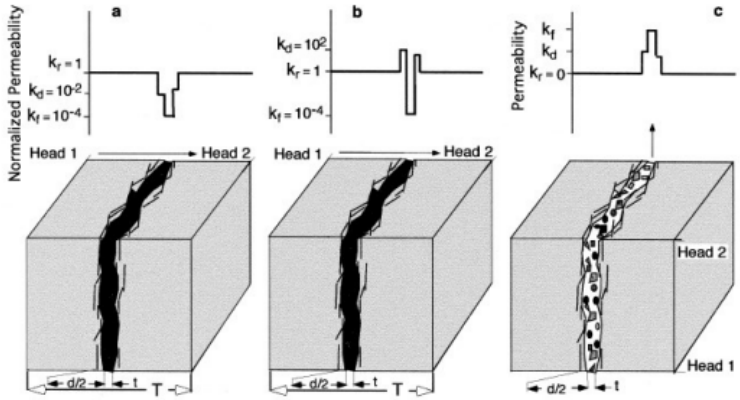

Figure 3: Three situations for a normalized permeability along a fault zone. A shows a deformation band zone, which decreases the permeability. B shows a fault created by shearing. The fault rock is surround by a permeable damage zone. C shows a fault zone containing breccia which results in increased permeability (Rawling et al., 2001).

In the deformation bands of sandstone, the permeability in a fault usually decreases, due to the much smaller grain size, poorer sorting, and a lower porosity in the deformation bands than the original sandstone (R. Schultz, 2009). Sandstones mostly have high fault densities, faults in a reservoir can reduce the permeability up to 80% (Fowles & Burley, 1994). In reality, the fault zone has various permeability values, in the model of this thesis an overall average value will be used for the fault.

In the model, $40*10^{-14}$ m^2 has been taken as permeability value of the reservoir. The permeability of sandstone faults can have many different values, dependent on the fault structures. Measured permeability values of faults of the Quartz Sandstones in Oklahoma ranged from 50^{-17} m^2 until 52^{-15} m^2 (E.D. Pittman, 1981), measured permeability values of faulted eolian sandstone of the Jurassic Navajo Sandstone ranged from 10^{-16} m^2 to 20^{-12} m^2 (Z.K. Shipton *et al*., 2002) and M. Antonellini & A. Aydin (1994) state that the permeability values of sandstone in the fault zone decreased to values of 10^{-19} to 10^{-16} m^2. Furthermore, Woodcock (1987) and Fowles & Burley (1994) also state that the permeability of a sandstone decreases around three orders of magnitude in a fault. In the model, the fault will have permeability values ranging from 10^{-17} m^2 to 10^{-11} m^2. The reservoir has a permeability of $40*10^{-14}$ m^2 and more than a contrast of 3 or 4 orders of magnitude will not be possible to calculate in this model, the reason will be explained in the discussion. Even though most of the times the permeability decreases in a fault in a sandstone reservoir, it is still interesting to see what happens when there is an increase in permeability, as then the influence of this parameter can be investigated even better.

2.2. Thickness

The thickness of a fault varies enormously. The entire fault zone, which can be very large, can have a different permeability than the surrounding rock and thus influences the flow of the reservoir. This zone can range from centimetres to hundreds of metres (Lin & Yamashita, 2013). In good quality sandstone reservoirs however, faults tend to be of small-scale due to the strength of the sandstone, which is proportional to its porosity (T. Manzocchi *et al*., 1998). As the reservoir of the model in this thesis is only 600 m by 300 m and the well spacing is 400 m, the fault will be modelled with thicknesses of 10 cm until 150 m.

2.3. Angle

Faults can theoretically have every angle, as it depends on the stress direction and on the fracture orientation. The stress direction, however, can be dependent on its location on earth which could result in a more common fault angle per area. Since the model is 2D, the type of fault and also the dipping angle has not been taken into account. The angle is modelled with values ranging from 0 to

90 degrees. At 0 degrees, the fault is perpendicular to the flow, at 90 degrees the fault is parallel to the flow.

2.4. Pressure Gradient

Paragraph 1.2 stated that after injection and production, a high-pressure gradient occurs at the wells. Also at a barrier of low permeability the pressure gradient will increase, which can be described with equation 1, derived from Darcy's law for fluid flow. The fluid velocity will stay the same at both sides of the barrier, which can be described on the basis of the mass balance: "what goes in, must go out". The viscosity is maintained as well. The permeability 'k' decreases at the boundary and since the flow rate 'v' is fixed, the pressure gradient increases. The higher the permeability difference of the barrier and the reservoir, the higher the pressure gradient will become.

$$v = \frac{k}{\mu}\frac{\Delta P}{\Delta x}$$

Equation 1: Derived from Darcy's law for flow. Velocity through permeable media in a one-dimensional homogeneous rock formation with a single fluid phase and a constant fluid viscosity

3. Method

The main goal of the thesis is to investigate the influence of fault parameters on the performance of a geothermal reservoir. Thus, a model must be made that represents a geothermal reservoir, including a well doublet and a fault. A basic and small 2D heat flow model without fault has been made in advance, with which the temperature and pressure at every point of the reservoir can be calculated at every time step. This model has then been adjusted during this project with various aspects: enlarging the reservoir, adding a fault and increasing the accuracy for example. During the modelling, the fault parameters will be varied for both a finite and infinite fault and finally the output, the pressure values and the temperature values, will be compared. In the following paragraphs, the setup of the model will be explained.

3.1. Finite Element Method

The model is numerical, based on the finite element method. The method solves a larger problem by dividing it in smaller parts (smaller equations): finite elements (D.L. Logan, 2011). These smaller parts will then be assembled into the larger system of equations and a solution is approximated by minimizing an associated error function.

To model the flow in the reservoir, properties and equations of every point in the reservoir must be taken into account. The reservoir is divided into grid blocks, it forms a mesh consisting of elements. Every element is then calculated separately and finally added to a total solution. The smaller the mesh size, the more accurate the solution will be. However, a smaller mesh size also means a longer calculation time. As said above, the approximate values of the elements are calculated at a discrete number of points over the domain: a sequence of time steps. Accuracy will be increased when there are more time steps, but this will also increase the computational time. Sufficiently small-time steps to reduce temporal errors must be used in order to obtain a time-accurate discretization of a highly dynamic flow problem (M. Moller, 2015). In this model 62 time steps are used, which represent a total of 50 years. The time steps start small, until the model approaches a year and from then on, the time step is a year until the end of the simulation.

In addition, the MATLAB function 'sparse' was used. In numerical models, the system is often loosely coupled. This means that the components have little or no influence on other components. Because of this, the matrix contains a lot of zeroes (a sparse matrix), which uses up a lot of memory. The sparse function in MATLAB eliminates all the zero elements, this increases the running speed.

3.2. Boundary Conditions

The finite element analysis requires boundary conditions, as a unique solution must exist to solve the equations. The boundary conditions limit the solutions at the boundaries at a certain value for every time step. This model has a 'no flow boundary condition' at the boundaries of the reservoir. The model is based on solving for Pressure and Temperature at each location and time step. At the sides of the reservoir there is no fluid flow and no heat flow. The velocity 'v' is proportional to the pressure 'ΔP' in equation 1 of Paragraph 2.4, so when there is no velocity, there is no pressure gradient. At the injection well, the boundary conditions are the injection temperature of 40 degrees and the fixed flow rate. At the production well, there is also a fixed flow rate, which is the same as at the injection well.

3.3. Mesh Generation

At the wells and fault, there is a very high pressure gradient, as explained in Paragraphs 1.1 and 2.4. At a very small distance x, the pressure P differs enormously, so the mesh must be really refined to be able to smoothly show the pressure distribution without showing overshoot and undershoot in

pressure and temperature output. However, to have a tiny mesh size in the whole reservoir takes up a lot of memory and is not necessary as the gradient is much lower away from the fault and wells. Thus, a mesh with very small elements at the fault and well and bigger elements in between, where it is of less significance, would be convenient. To generate a mesh that is not of uniform size and not evenly distributed over the reservoir, a MATLAB code called 'DistMesh' (P.O. Persson & G. Strang, 2004) was used. The 'Rectangle with circular hole, refined at circle boundary' and 'Square, with size function and line sources' have been implemented. The code is able to generate a mesh of unstructured triangular and tetrahedral shapes. All the geometries are specified by 'Signed Distance Functions'. These functions calculate the smallest distance between any point in the reservoir to the domain boundary (P.O. Persson & G. Strang, 2004). In Figure 4 the mesh that is used in the modelling is displayed, it can be clearly seen that the mesh size at the wells and the fault is significantly smaller compared to the rest of the reservoir. The well on the left is the injection well and the well on the right is the production well. At the left part of the reservoir, another refinement has been made in order to prevent overshoot and undershoot at the injection well. This part of the MATLAB code can be found in Appendix 1.

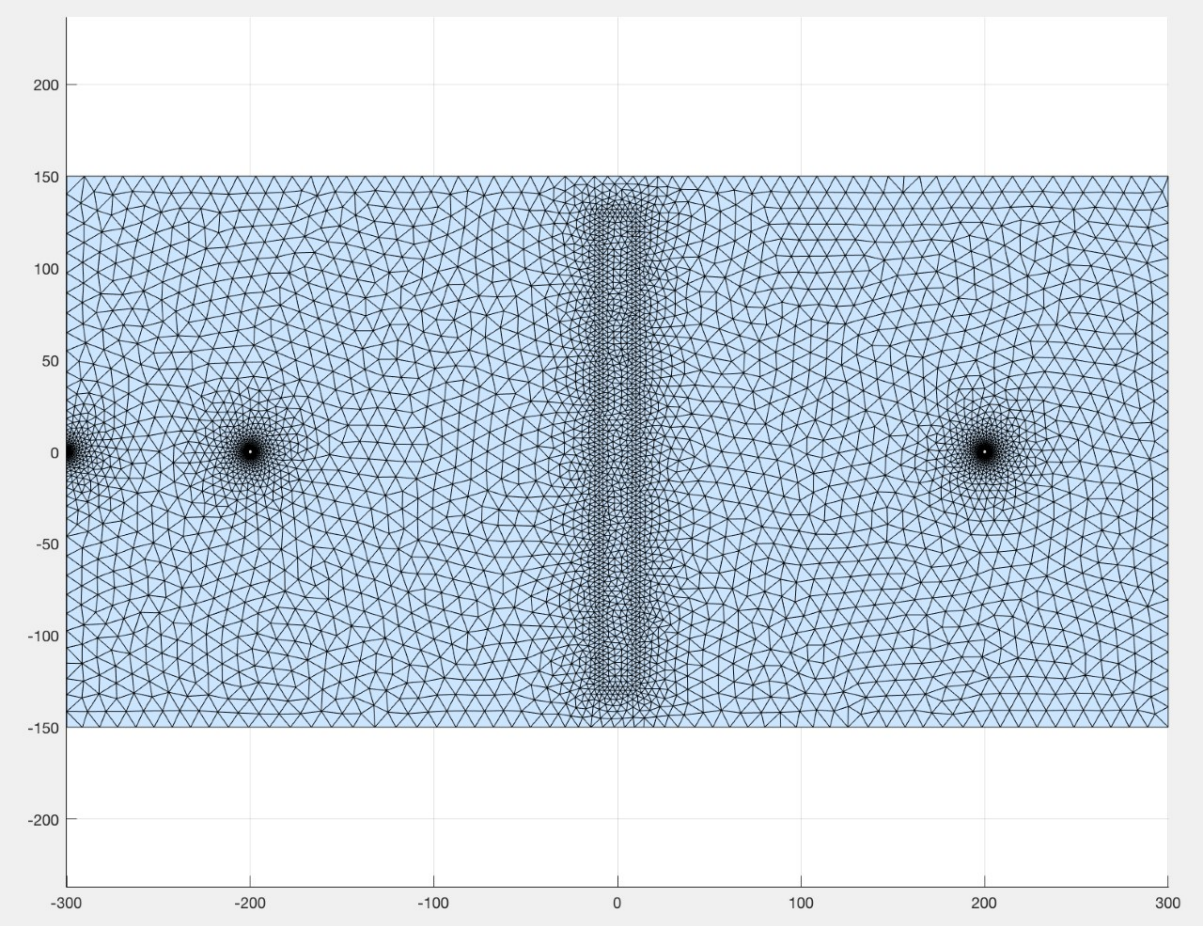

Figure 4: The mesh generated in MATLAB with the DISTMESH function (P.O. Persson & G. Strang, 2004) with the well doublet and the fault. At x=-300, y=0, another refinement has been made in order to prevent overshoot and undershoot near the injection well.

3.4. Mesh Sensitivity Analysis

A fine mesh grid results in accurate solutions, however it is very time-consuming. An analysis of the mesh size must be made, in order to generate a mesh that is accurate enough, while having the highest possible running speed. Three different parameters of the mesh generation have been analysed: the

maximum edge length of the whole mesh grid, the well edge length and the growth rate of the mesh triangle.

A 'for loop' has been made in MATLAB with maximum edge lengths varying from 80 to 5. The average temperature results at the production well for those maximum edge lengths have been displayed in Figure 5. It can be seen that the temperature at a time step can differ more than 3 degrees depending on the maximal edge length, so this value is of big influence on the result. A lot of lines are overlapping at a certain height; the temperature is not influenced very much anymore at certain maximal edge lengths. After zooming in and testing another few times, the temperature outcome becomes stable and does not have an undershoot or overshoot at a maximal edge value of 10, thus this will be the maximal edge length of the mesh used in the model. After this, the well edge length has been tested, in the same way as the maximal edge length. This is the mesh size at the radius of the wells. A 'for loop' has been made for well edge lengths ranging from 0.5 to 0.05. At a well edge length of 0.35 the results became stable. Thirdly, the growth rate is tested. With a maximum edge length of 10, a well edge length of 0.35 and a growth rate of 0.2 the temperature results show no over and/or undershoot and the changes when using smaller values become insignificantly small.

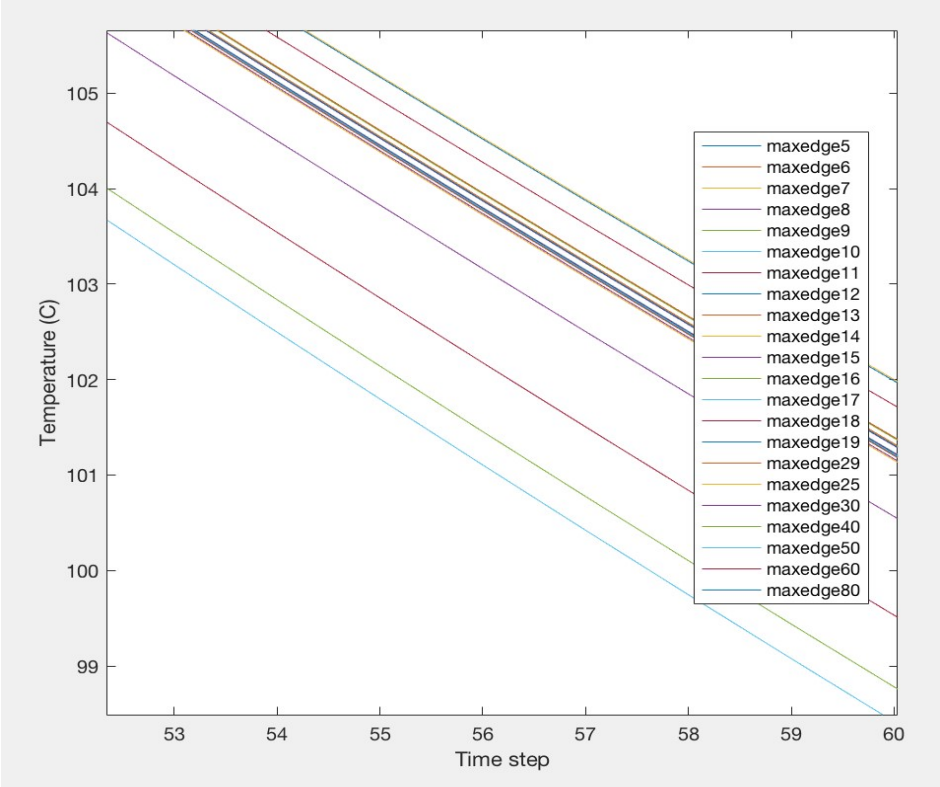

Figure 5: A plot created in MATLAB of the temperature at a few time steps with different maximal edge lengths.

3.5. Impedance

As explained in Paragraph 1.2, a higher impedance requires a higher pumping power, and thus higher operational costs, therefore it is important to investigate the influence on the pressure. With a fixed flow rate and viscosity, a lower permeability results into a higher impedance, which can be described on the basis of equation 2, Darcy's law for fluid flow.

$$Q = \frac{k_{avg} * w * h * \Delta P}{\mu * L}$$

Equation 2: Darcy's law for fluid flow with discharge 'Q', average permeability 'k_{avg}', width 'w', thickness 'h', pressure difference 'ΔP', viscosity 'μ' and length 'L'.

The model in MATLAB shows a pressure distribution after each time step. However, the fault sometimes causes too small differences in impedance to see it clearly with the naked eye on the colour bar. Therefore, the impedance of the reservoir at different situations will be calculated using equation 2. The average permeability will be estimated by using the 'weighted-average permeability' method. This estimation is just for seeing the influence of the fault parameters on the impedance. The accurate calculation of average reservoir permeability is much more complicated. For calculating the weighted-average permeability, the reservoir has been divided into three zones, which have been displayed schematically in figure 6. As the fluid in the whole reservoir has the same flow rate and viscosity, the average permeability of zone 2 can be derived with equation 3. The total pressure difference is equal to the sum of the pressure drops across each zone.

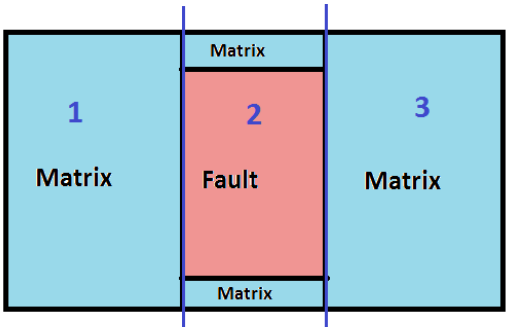

Figure 6: Schematic figure of reservoir divided into three zones.

$$k_{avg} = \frac{k_1 w_1 + k_2 w_2 + k_3 w_3}{w_t}$$

Equation 3: weighted average permeability equation

4. Experiment Sets in MATLAB

As explained before, the reservoir has been modelled with different fault variables: fault thickness, permeability and angle. They have all been calculated by using a 'for loop' with all the different values. While varying one of the three variables, the other two have been kept fixed. During the investigation of the influence of the fault permeability and thickness, also an infinite fault has been modelled to compare the results. As the fluid is not able to bypass the fault with an infinite fault, the results should be significantly different. Below the calculations are explained shortly. The reservoir has a size of 600 m x 300 m and a well spacing of 400 m and the finite fault has a length of 260 m.

4.1. Fault Permeability

First of all, the permeability parameter has been varied to decide a base value for the permeability of the fault. It is convenient to use a fault permeability that has a significant influence on the reservoir, as then the dependence on thickness and angle can be seen more easily. The fault has been given a different permeability than the surrounding area by using the function 'inpolygon', which indicates whether certain points are in or outside a certain area. If the element is inside that area, it receives the value of the fault permeability and if it is outside that area, it receives the reservoir permeability value. The permeability of the reservoir is $40*10^{-14}$ m^2 and the permeability of the fault ranges from 10^{-11} m^2 until 10^{-17} m^2. The base value of fault permeability will be 10^{-14} m^2, in the next chapter it will be clear how this value has been chosen.

4.2. Fault Thickness

The thickness of the fault in the model varies from 10 cm until 150 m. This has been done by varying the x coordinates of the fault mesh with every loop. 20 m has been chosen as the base thickness for the fault.

4.3. Fault Angle

The angle of the fault has been varied by multiplying the fault coordinates with the rotation matrix (equation 4). The angle (theta) has been varied from 0 to ½ π. At zero the fault is placed perpendicular to the flow. At ½ π, the fault has turned parallel to the flow. In Appendix 2 a generated mesh of the reservoir with a fault with an angle of 45 degrees is shown as an example. The base value for the angle is zero degrees, so the fault perpendicular to the flow.

$$R(\theta) = \begin{bmatrix} \cos\theta & -\sin\theta \\ \sin\theta & \cos\theta \end{bmatrix}.$$

Equation 4: Rotation matrix (Familton, 2015).

5. Results

The production temperatures were determined by finding the elements in MATLAB that had the same coordinates as the well location and taking the average of their solutions. The impedance has been estimated by using the method described in Paragraph 3.5.

First, a reservoir without fault has been modelled to check the temperature and pressure behaviour without the fault influence. In Figure 7, the plots for the pressure and heat flow after 50 years are displayed. In Figure 8, a graph of the temperature throughout the reservoir after 50 years is presented. In this situation, the fluid tries to directly reach the production well, due to the pressure difference, and has no obstacles of lower permeability values. The final temperature after 50 years is 100.6 degrees and the impedance has been approximated 1.7 MPa. In the following paragraphs the significant results of the three tested fault parameters are presented.

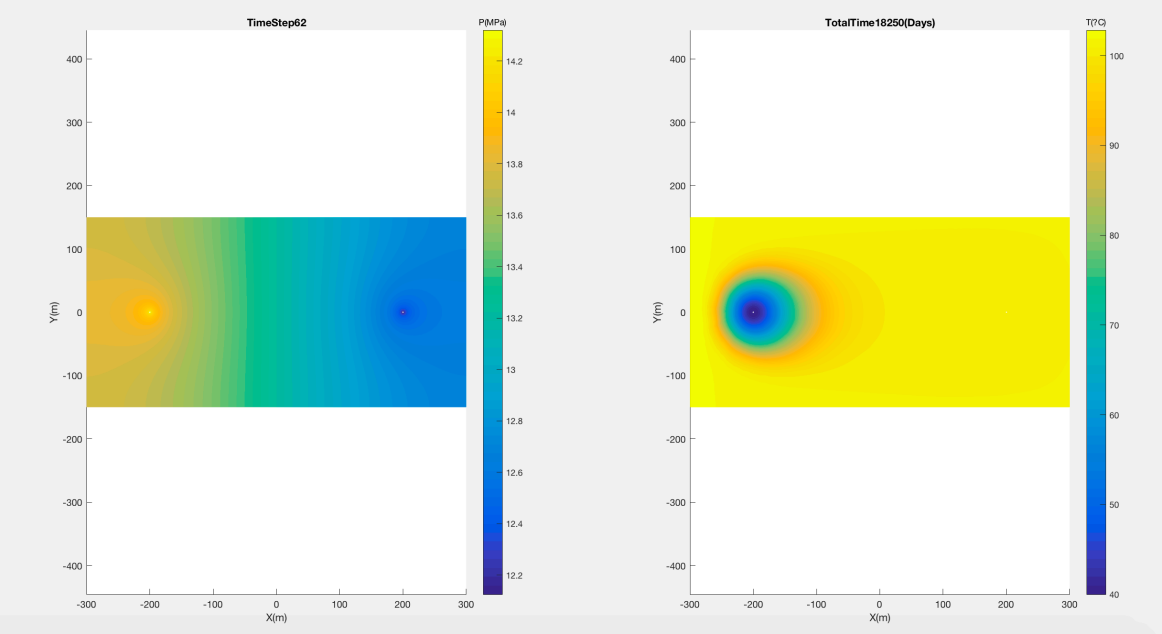

Figure 7: Pressure distribution and heat flow of the reservoir without fault after 50 years

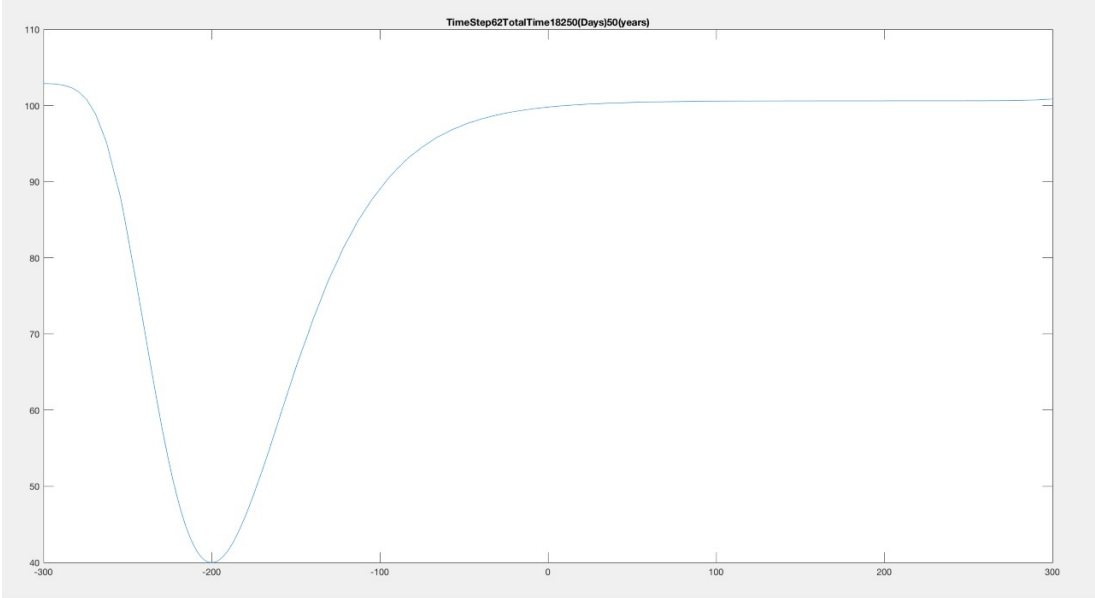

Figure 8: Plot of the temperature throughout the reservoir after 50 years

5.1. Fault Permeability

Temperature

The trend of the production temperatures at a few fault permeability's has been displayed in Figure 9. Increasing the permeability of the fault, does not have a lot of influence on the reservoir. This might be due to the fact that the fluid will follow the same path as without fault in the direction of the production well, due to pressure difference. Decreasing the permeability of the fault, does lead to a significant higher production temperature. At a slight decrease of the permeability, the final temperature slowly rises. The fluid will start to bypass the fault and sweep away the warmth of the sides of the reservoir towards the production well. The fluid will cover a larger distance on its way to the reservoir, consequently it will extract a larger amount of heat. At a fault permeability of 10^{-14} m^2, the final temperature suddenly shows a larger increase and it becomes constant. Now the permeability of the fault is low enough for all the fluid to bypass the fault. From this value on, the fluid seems to have reached all the sides from the reservoir and swept away all the warmth, since a lower permeability does not have any further influence.

With an infinite fault, the production temperature only increases (with 5 degrees) at a fault permeability of 10^{-16} m^2. The fluid still goes to the production well, but will first distribute over the length of the fault, and consequently reach more reservoir area before reaching the production well. With further decreasing permeability the temperature does not change, however, much smaller values could not be calculated as the difference with the matrix permeability was too large.
The complete table of production temperatures at different fault permeability's is given in Appendix 3.

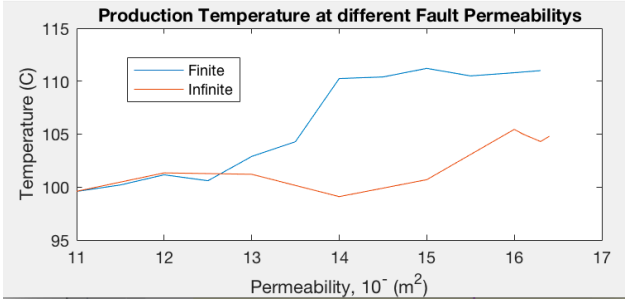

Figure 9: production temperature at permeability's ranging from 10^{-11} to 10^{-17} m^2

Impedance

The calculated values for the impedance can be found in Appendix 4 and the trend can be seen in Figure 10. Only six values have been calculated, therefore it is not a smooth line, but to be able to follow the trend more values are not necessary.

The impedance of the finite fault at a fault permeability of 10^{-14} m^2 is estimated 2.0089 MPa. This is a slightly higher value than the case without fault. Apparently an additional pressure of 0.3 MPa must be applied to overcome the impedance in that case. A fault permeability of 10^{-17} m^2 creates an impedance of 2.0683 MPa. So decreasing the fault permeability does also not have a lot of further influence on the impedance, just like at the temperature, as the fluid seems to already have bypassed the fault completely at a fault permeability of 10^{-14} m^2. With the impedance being clearly inside the threshold of 10 MPa, in which the required pumping powers should be acceptable, the lower fault permeability's might be an advantage for the feasibility of the reservoir.

An infinite fault gives an impedance of 3.91 MPa at a fault permeability of 10^{-14} m^2, an impedance of 24.31 MPa at a permeability of 10^{-15} m^2 and 228.31 MPa at 10^{-16} m^2. The fluid has no choice than to go through the fault, and consequently a higher pressure drop must be overcome. The higher production temperature at a permeability of 10^{-16} m^2 does by far not weigh against the amount of pumping power necessary.

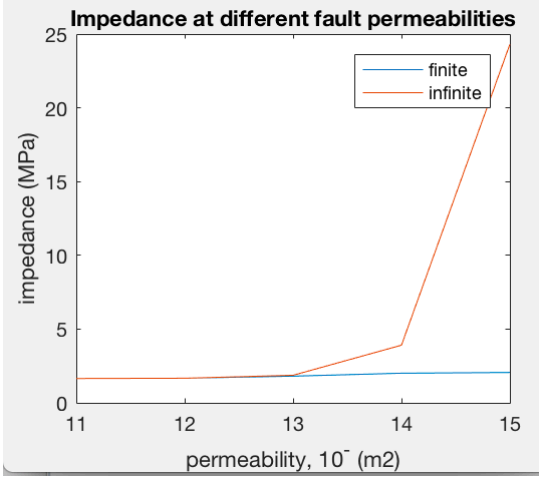

Figure 10: Impedance at permeability's ranging from 10^{-11} – $10^{-15}m^2$

5.2. Fault Thickness

Temperature

In Figure 11 can be seen that at a fault thickness of 20 m, which is also the base value, the production temperature has the highest value compared to other thicknesses. This thickness clearly has the best sweeping effect. At a very low thickness, the fault does not have a major impact over the circulation period so the results are comparable with a faultless reservoir. But with a very large thickness, in this model already at a thickness of 30 m and more, the sweeping effect will not weigh against the unrecoverable area of the fault. The fluid then bypasses the fault and is unable to recover the heat in the fault. With an infinite fault, the fluid decreases quickly, as it seems unable to reach the complete fault area. The production temperature at each thickness is listed in Appendix 5.

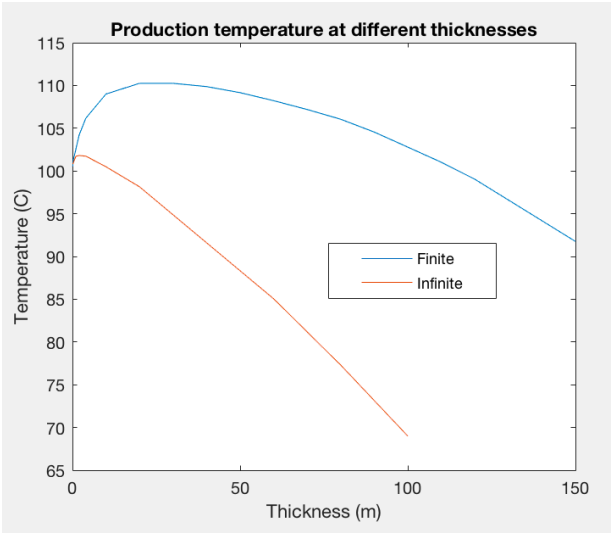

Figure 11: the production temperature at different thicknesses for a finite and infinite fault

Impedance

As stated in the previous paragraph, the impedance at a thickness of 20m had an estimated value of 2 MPa. Figure 12 shows that the impedance increases linearly with increasing thickness. A fault thickness of 40 m leads to an impedance of 2.3 MPa for example and a fault thickness of 150 m leads to an impedance of 4 MPa. Both values are still in the threshold of 10 MPa, so the pumping power needed can be overseen. An infinite fault, however, already leads to an impedance of 6.12 at a thickness of 40m and an impedance of more than 10 MPa at 80 m. The impedance values are listed in Appendix 6.

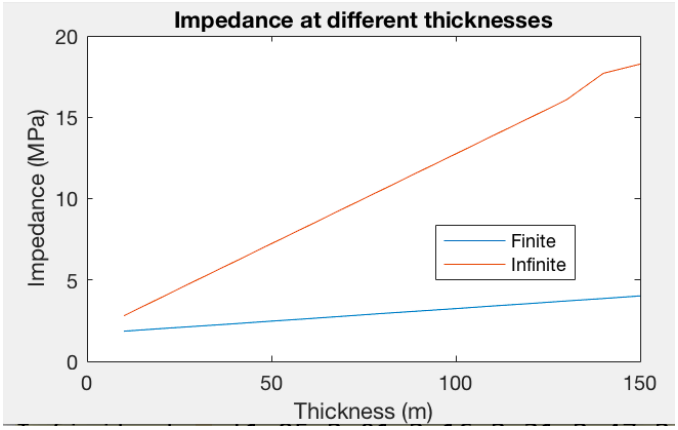

Figure 22: Impedance at different thicknesses for a finite and infinite fault

5.3. Fault Angle

The temperature shows a clear decline when turning the fault to a position from perpendicular to parallel to the fluid flow. When the fault is perpendicular to the fluid flow, a big amount of fluid will bypass the fault and thus sweep all the heat from the sides of the reservoir. A parallel position of the fault causes the fluid to go almost straight to the production well and the temperature and pressure will have a similar outcome as a reservoir without fault. At a complete parallel position, the temperature even becomes a little bit lower (99,7 degrees) than the temperature without fault (100.6 degrees). This is probably due to the fact that the flow still almost goes completely straight to the production well, however there is an area of 260 x 20 m of unrecoverable heat that will not be extracted.

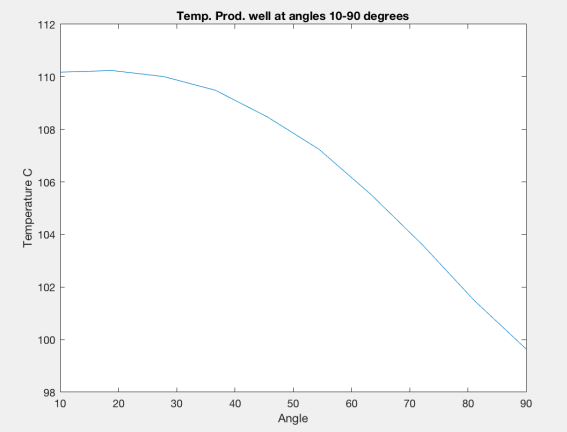

Figure 13: Plot of the final temperature at the production well at different fault angles

.

6. Conclusion

The main purpose of this research was to investigate the influence of fault permeability, thickness and angle on the temperature and pressure performance of a geothermal reservoir. From the results that were obtained, it can be seen that all three fault parameters have significant influence on the temperature behaviour of the reservoir, at both an infinite and finite fault, as they can all maximize and minimize the influence of the fault on the reservoir. At a finite fault, the major impact of the fault is the direction of the fluid flow in the reservoir. Increasing the fault permeability leads to a higher temperature outcome at the production well, as the fluid bypasses the fault and will travel through a larger part of the reservoir and thus extract a larger volume of heat. The fault angle is able to cancel the influence of the fault, as at a parallel position the reservoir behaves the same as without fault. Increasing the thickness of the fault first leads to a higher temperature outcome due to the sweeping effect, but after a certain thickness, the temperature at the production well decreases due to the large amount of unrecoverable area, which makes it unable for the fluid to reach all the heat in the reservoir. An infinite fault has less influence on the production temperature and only gives a small increase of temperature at a very low permeability.

The impedance does not have a significant influence at a non-infinite fault as the fluid can apparently easily bypass the fault. At an infinite fault, the impedance keeps building up with a decreasing permeability and increasing thickness, far beyond the acceptable threshold of 10 MPa.

A lower permeable finite fault clearly can have a positive influence on the reservoir behaviour. The sweeping and bypassing of the fault causes a higher production temperature, with the impedance staying within the threshold of 10 MPa. Consequently, this means a larger energy production of the geothermal system. A very low permeable infinite fault also increases the production temperature, as the fluid tries to go through the fault over an as large area of the fault as possible. However, the higher production temperature does by far not weigh against the large amount of pumping power needed to overcome the pressure drop. As sandstones usually have lower fault permeability's, an infinite fault will probably cause the reservoir to be unprofitable.

This knowledge of how the fault parameters affect the temperature and pressure behaviour of a geothermal reservoir, can now be taken into account when developing new well doublets in faulted areas. This will increase the ability of predicting the performance of the reservoir and that means thus another step in reducing the role of uncertainties, that currently make justifying geothermal projects so difficult.

7. Discussion

The accuracy of the model has been improved by doing the mesh analysis, which is explained in Paragraph 3.4. The maximal edge length, well edge length and growth rate of the mesh grid, have all been analysed by making for loops with different values for these three parameters. The final values have been determined by examining the differences of the temperature at the production well at the last time steps, and by checking for overshoot and undershoot of the temperature during the modelling. Using smaller values for these three parameters did not improve the model, the results remained constant.

The model does have some limitations. First of all, while using smaller mesh parameter values did not improve the model, the temperature outcome when running the model multiple times with the exact same values is not precisely constant. A difference of approximately 0.2 degrees has been experienced, which presumably could be solved by even further mesh refinement, or it is influenced by other unknown factors. However, it did not affect the conclusion of this report as that was a comparison study based on larger differences.

Secondly, when the contrast between the permeability of the fault and the permeability of the sandstone matrix increases, also a more and more fine mesh is needed as explained in Paragraphs 2.4 and 3.3. Only three orders of difference with the matrix permeability could be calculated with the model of this thesis, using higher and lower values resulted into over and undershoot. For more contrast, extreme refinement is required, which is impossible to implement on a normal computer as the size of the Random-Access Memory is too small. Above aspects suggest a more powerful computer and a larger amount of time.

To decrease computation time, a symmetrical model (with the centreline halfway through the reservoir connecting both wells) could have been used so only half of the reservoir had to be modelled with a no-flow boundary condition at the interface. This is only applicable if both halves are homogenous, so it would have been possible to implement it in this thesis when modelling for the fault permeability and thickness. This would have been convenient in order to investigate even more parameters, especially considering the small amount of time scheduled for this research. However, the realization of the possibility to use the symmetrical model came in a too late stage of the research to be of any advantage.

Moreover, a 2D model has been used in this research. M. Antonellini and A. Aydin (1994) state that it is important to use a 3D model when evaluating fluid flow through a low-permeability fault zone, because it has to be done at an appropriate scale for the problem and is needed to correctly evaluate sealing properties of faults for example. Especially large faults come with various structures such as slip surfaces, deformation bands, breccia zones, etc. which are arranged in a complex 3D structure.

Also, the reservoir in the model is assumed to be homogeneous. To obtain a more realistic solution, heterogeneous rock formations must be incorporated as the reservoir is not likely to have the same properties everywhere. For example, deformation bands throughout the reservoir can have a significant influence on the fluid flow (R. Schulz, 2009). This also counts for the fault. As said before, the fault zone consists of different structures which do not have a uniform value. Also, the same applies for the fault geometry, besides it being 2D, it is also modelled with straight lines which perhaps simplifies the calculation too much. Actual fault geometries should be incorporated for a more detailed evaluation and the realistic petrophysical values of all those structural aspects of the fault should be used (M. Antonellini & A. Aydin, 1994).

Furthermore, faults can form permeable parallel pathways coming from great depths to shallower aquifers and reservoirs (E.C.D. Hooper, 1991). The parallel permeability can be one order of magnitude bigger than the perpendicular permeability (M. Antonellini & A. Aydin, 199). This can cause a warm water supply from greater depth. This can also cause reservoir fluids to accommodate along the fault upward, out of the reservoir, due to the density difference. That the fault can act like a parallel pathway from and into other layers, has not been taken into account during the modelling.

8. Recommendations

For further research about this topic, a model could be built with a heterogeneous reservoir. Therefore, data of a reservoir with fractures, different (fault) permeability values, different densities, different rock properties etc. should be implemented. Also, a 3D model would present a more realistic solution. Moreover, the anisotropy could be taken into account in the future. In this model, no difference has been made between permeability values in different directions. Particularly when a model is in 3D, which would be an improvement, it is important to take into account the anisotropy, as especially the permeability in vertical direction can vary significantly from the permeability in the horizontal directions. Furthermore, now only one fault has been investigated, it would be interesting to do the research with more faults and vary their permeability values to see the influence on the reservoir. In addition, researching the possibility of a fault enabling fluids to flow from and into other layers, by acting as a pathway, would be a useful addition as well.

References

C.J.L. Willems, H.M. Nick, D.F. Bruhn, *The impact of reduction of doublet well spacing on the Net Present Value and the life time of fluvial Hot Sedimentary Aquifer doublets*, Ph.D. thesis, Faculty of Civil Engineering and Geosciences, Delft University of Technology *(2017)*

R.C.A. Smit, *Optimization of geothermal well doublet placement*, MSc. Thesis, Faculty of Civil Engineering and Geosciences, Delft University of Technology *(2012)*

K. Nicholson, *Geothermal Fluids – Chemistry and Exploration Techniques*, ISBN-12: 978-3-642-77846-9, Springer-Verlag Berlin Heidelberg *(1993)*

T. Manzocchi, P.S. Ringrose, J.R. Underhill, *Flow through fault systems in high-porosity sandstones*, Geological Societey London, Special Publications **127**, 65-82 *(1998)*

Lukawski, M.Z., Anderson, B.J., Augustine, C., Capuano, L.E., Beckers, K.F., Livesay, B. and Tester, J.W., 2014. *Cost analysis of oil, gas, and geothermal well drilling*, Journal of Petroleum Science and Engineering **118**, 1-14 *(2014)*

A. Hjartarson, *Heat Flow in Iceland*, Iceland GeoSurvey, Proceedings World Geothermal Congress, Melbourne *(2015)*

H.A. Van Adrichem Boogaert, W.F.P. Kouwe, *Stratigraphic Nomenclature of the Netherlands*, Netherlands Institute of Applied Geosciences TNO – National Geological Survey, *(1993-1997)*

NLOG, *LIR-45*, retrieved from http://www.nlog.nl/nlog/requestData/nlogp/allBor/metaData.jsp?tableName=BorLocation&id=106507505

D. Bonte, J.D. van Wees, J.M. Verweij, *Subsurface temperature of the onshore Netherlands: new temperature dataset and modelling*, Geological Survey of the Netherlands, Utrecht*, (2012).*

M. Antonellini, A. Aydin*, Effect of faulting on fluid flow in porous sandstones: Geometry and spatial distribution*, AAPG bulletin **78**, 355-377, *(1994)*

G. C. Rawling, L.B. Goodwin, J.L. Wilson, *Internal architecture, permeability structure and hydrologic significance of contrasting fault-zone types*, Geology **29 –** 1, 43-46, *(2001)*

J. Fowles, S. Burley, *Textural and permeability characteristics of faulted, high porosity sandstones,* Marine and Petroleum Geology **11** - 5, 608-623, Elsevier, *(1994)*

J. Bear, *Dynamics of Fluids in Porous Media* (**1**), American Elsevier Publishing Company, *(1972)*

K. Yamashita, A. Lin, *Spatial variations in damage zone width along strike-slip faults: An example from active faults in southwest Japan*, Journal of Structural Geology **57**, 1-15, *(2013)*

R. Schultz, *Fractures and Deformation Bands in Rock: A Field Guide and Journey into Geologic Fracture Mechanics*, Oxford University Press, *(2009)*

R.C.M. Malate, J.J.C. Austria, *Matrix stimulation treatment of geothermal wells using sandstone acid*, Stanford University, California *(1998)*

D.L. Logan, *A first course in the finite element method*, Cengage Learning, ISBN 978-0495668251, *(2011)*

M. Moller, *Time stepping methods*, [PowerPoint Slides], Retrieved from http://ta.twi.tudelft.nl/nw/users/matthias/teaching/athens/timestepping_2015.pdf , Delft University of Technology, *(2015)*

P.O. Persson, G. Strang, *A Simple Mesh Generator in MATLAB*, SIAM Review **46**, 329-345, *(2004)* DistMesh code retrieved from http://persson.berkeley.edu/distmesh/

J.S. Caine, J.P. Evans, C.B. Forster, *Fault zone architecture and permeability structure*, Geology **24** - 11, 1025–1028, *(1996)*

E.D. Pittman, *Effect of Fault-Related Granulation on Porosity and Permeability of Quartz Sandstones*, Simpson Group (Ordovician), AAPG Bulletin **65** - 11, 2381 – 2387, *(1981)*

Z.K. Shipton, J.P. Evans, K.R. Robeson, C.B. Forster, S. Snelgrove, *Structural heterogeneity and permeability in faulted eolian sandstone: Implications for subsurface modelling of faults*, AAPG Bulletin **86** - 5, 863-883, *(2002)*

E.C.D. Hooper, *Fluid Migration Along Growth Faults In Compacting Sediments*, Journal of Petroleum Geology **14**, 161-180, *(1991)*

B. Steingrimsson, *Geothermal Well Logging: Temperature And Pressure Logs*, Iceland GeoSurvey, *(2013)*

Appendix

Appendix 1:
Matlab code for the mesh generation:
DistMesh function retrieved from http://persson.berkeley.edu/distmesh/ (P.O. Persson & Gilbert Strang, 2004)

```
% input data
% cd(pwd)
%  cd('/Users/ylanavanhout/Downloads/New folder2/');
prnt_fold = pwd;
%
%  addpath('/Users/ylanavanhout/Downloads/New folder/Distmesh/distmesh');

cd(pwd);
addpath(genpath(pwd))


%create for loop over whole script to measure mesh sensitivity. However you
%want to keep the average T so use clearex

%k_a = 20:-1:5;
%k_c = 0.5:-0.05:0.05;
%k_d = 0.6:-0.05:0.1;
%for iteration_maxedgelength=1:numel(k_a)
%for iteration_edgelengtharoundwell = 1:numel(k_c)
%for iteration_growthrate = 1:numel(k_d)
%clearvars -except Avrge_prod_T k_d iteration_growthrate prnt_fold

%k_w = [0.1,0.2,2,4,10,20,30,40,50,60,70,80,90,100,110,120,150];
%for iteration_width = 1:numel(k_w)
%clearvars -except Avrge_prod_T k_w iteration_width prnt_fold

% Mesh with two wells and fault
clc
%edge_length_around_well= k_c(iteration_edgelengtharoundwell);
edge_length_around_well = 0.25; % smaller --> smaller mesh around well
edge_length_fault=2.5; % bigger --> smaller mesh around well
rad_well=1;
growth_rate = 0.2;
%growth_rate= k_d(iteration_growthrate);

%max_edge_length = k_a(iteration_maxedgelength);%20*0.8.^(k_a-1)
max_edge_length = 10


%well location
xc_left=-200;
yc_left=0;
xc_right=200;
yc_right=0;
```

```
%Reservoir size
X1_Res=-300;
X2_Res=300;
Y1_Res=-150;
Y2_Res=150;

Rect_fixed=[X1_Res,Y1_Res;X1_Res,Y2_Res;X2_Res,Y1_Res;X2_Res,Y2_Res];

%Fault coordinates:
X1_fault=10 %k_w(iteration_width);
X2_fault=-X1_fault;
X3_fault=X2_fault;
X4_fault=X1_fault;

%Infinite, otherwise 130
Y1_fault=-150;
Y2_fault=-150;
Y3_fault=150;
Y4_fault=150;

Point1=[X1_fault;Y1_fault];
Point2=[X2_fault;Y2_fault];
Point3=[X3_fault;Y3_fault];
Point4=[X4_fault;Y4_fault];

%Fault coordinates matrix
Fault_coordinates = [Point1,Point2,Point3,Point4];


%phi = linspace(pi/20,pi/2,10);
%phi = [pi/4]
%for iteration_rotation = 1:numel(phi);

%   clearvars -except iteration_rotation

%     Rot_matrix(:,:,iteration_rotation) = [cos(phi(iteration_rotation)),-
sin(phi(iteration_rotation));sin(phi(iteration_rotation)),cos(phi(iteration_rotatio
n))];
%      new_rotPoints(:,:,iteration_rotation) =
Rot_matrix(:,:,iteration_rotation)*Fault_coordinates;

% assign XY_fault
%new_rotPoints(1=x 2=y,point,iteration_rotation)
% X1_fault = new_rotPoints(1,1,iteration_rotation);
% X2_fault = new_rotPoints(1,2,iteration_rotation);
% X3_fault = new_rotPoints(1,3,iteration_rotation);
% X4_fault = new_rotPoints(1,4,iteration_rotation);
%
% Y1_fault = new_rotPoints(2,1,iteration_rotation);
% Y2_fault = new_rotPoints(2,2,iteration_rotation);
% Y3_fault = new_rotPoints(2,3,iteration_rotation);
% Y4_fault = new_rotPoints(2,4,iteration_rotation);


%Fault spacing
```

```
fault_spacing = edge_length_fault;

distance_12 = sqrt((abs(X2_fault-X1_fault))^2+(abs(Y2_fault-Y1_fault))^2);
distance_23 = sqrt((abs(X3_fault-X2_fault))^2+(abs(Y3_fault-Y2_fault))^2);
distance_34 = sqrt((abs(X4_fault-X3_fault))^2+(abs(Y4_fault-Y3_fault))^2);
distance_41 = sqrt((abs(X1_fault-X4_fault))^2+(abs(Y1_fault-Y4_fault))^2);

nr_steps_hor = distance_12/fault_spacing;
nr_steps_ver = distance_23/fault_spacing;

%Fault fixed points:
Fault_fix_12 = [linspace(X1_fault,X2_fault,nr_steps_hor);
linspace(Y1_fault,Y2_fault,nr_steps_hor)];
Fault_fix_12 = Fault_fix_12';

Fault_fix_34 = [linspace(X4_fault,X3_fault,nr_steps_hor);
linspace(Y4_fault,Y3_fault,nr_steps_hor)];
Fault_fix_34 = Fault_fix_34';

Fault_fix_23 = [linspace(X2_fault,X3_fault,nr_steps_ver);
linspace(Y2_fault,Y3_fault,nr_steps_ver)];
Fault_fix_23 = Fault_fix_23';

Fault_fix_41 = [linspace(X4_fault,X1_fault,nr_steps_ver);
linspace(Y4_fault,Y1_fault,nr_steps_ver)];
Fault_fix_41 = Fault_fix_41';

Fault_fixed = [Fault_fix_12;Fault_fix_34;Fault_fix_23;Fault_fix_41];

fd=@(p) ddiff(
drectangle(p,X1_Res,X2_Res,Y1_Res,Y2_Res),dunion(dcircle(p,xc_left,yc_left,rad_well
), dcircle(p,xc_right,yc_right,rad_well)) );
fh=@(p)min(   min(   min(...

min(edge_length_around_well+growth_rate*dcircle(p,xc_left,yc_left,rad_well),
edge_length_around_well+growth_rate*dcircle(p,xc_right,yc_right,rad_well))...

,edge_length_around_well+growth_rate*abs(dpoly(p,[X1_Res, yc_left;
X1_Res,yc_left]))...
                          )...

,edge_length_fault+growth_rate*abs(dpoly(p,[X1_fault,Y1_fault;
X2_fault,Y2_fault;X3_fault,Y3_fault; X4_fault, Y4_fault; X1_fault,Y1_fault]))...
                  )...
               ,max_edge_length...
           );


[p,t]=distmesh2d_mod2(fd,fh,edge_length_around_well,[X1_Res,Y1_Res;X2_Res,Y2_Res],[
Fault_fixed;Rect_fixed]);

axis on
size(p,1)

mesh_nodes = p;
```

```
mesh_elements = t;

%mesh_nodes_test{i}(:,:) = p;
%mesh_elements_test{i}(:,:) = t;
%end

%take all the means of the elements
elem_mean=[];
for tmp_elem=1:size(t,1)
    elem_ind=t(tmp_elem,:);
    elem_mean=[elem_mean;mean(p(elem_ind,:))];
end


out2=mesh_nodes';
fid = fopen(strcat('mesh_nodes.dat'), 'w');
fprintf(fid, '          %d          %d\n', out2);
fclose(fid);

out2=mesh_elements';
fid = fopen(strcat('mesh_elements.dat'), 'w');
fprintf(fid, '          %d          %d          %d\n', out2);
fclose(fid);
```

Appendix 2: mesh with a fault turned 45 degrees

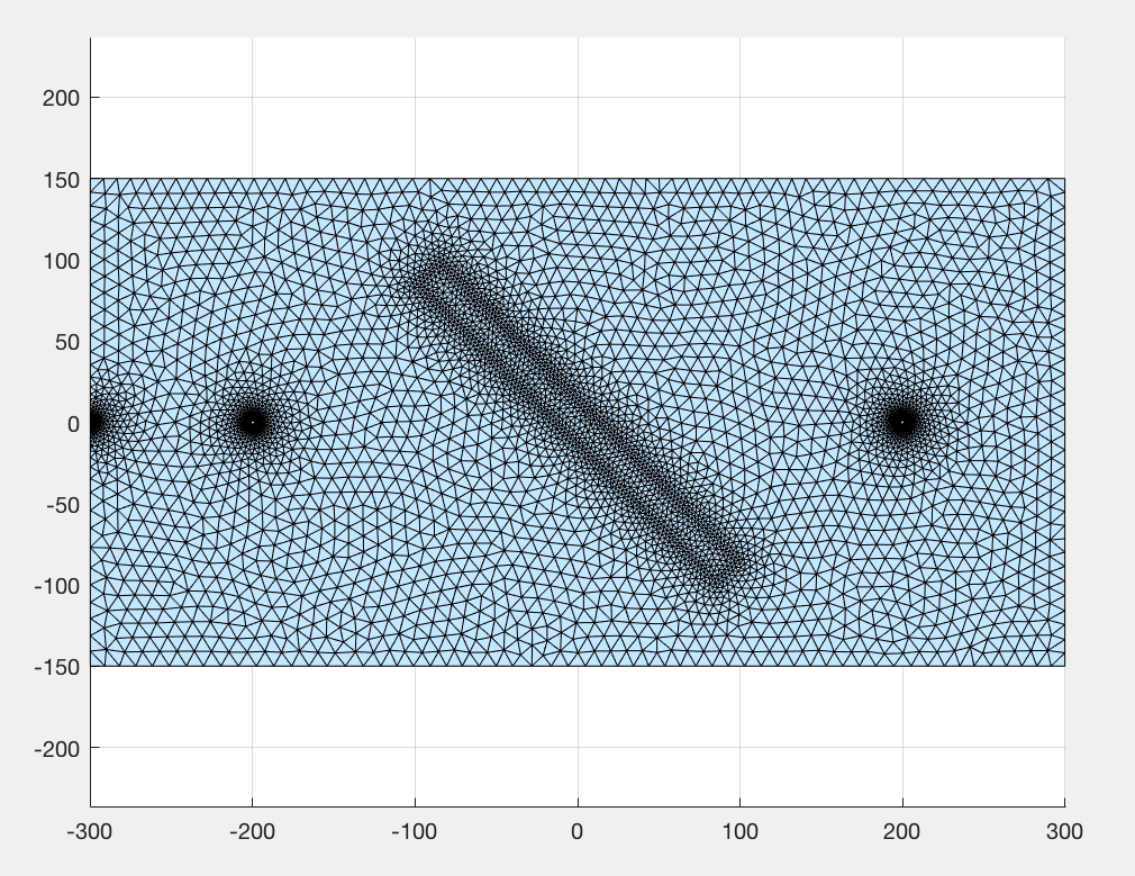

Appendix 3: Table with the production temperatures at different fault permeability's for a finite fault

Fault permeability m^2	Production Temperature C (finite fault)	Production Temperature (infinite fault)
10e-12	99,59	99,6
70e-13	99,76	
50e-13	100,20	
30e-13	100,91	
10e-13	101,16	101,34
90e-14	100,91	
60e-14	100,59	
40e-14	100,59	
10e-14	102,89	101,21
90e-15	102,97	
70e-15	103,55	
50e-15	104,29	
30e-15	105,96	
10e-15	110,25	98,1
90e-16	110,60	
10e-16	111,21	100,7
10e-17	110,8	105,45
5e-17	110,72	104,3

Appendix 4: Table with impedance values at different permeability's for finite and infinite fault with thickness of 20 m

Permeability m2	MPa (Finite)	MPa (Infinite)
10e-12	1,65	1,65
10e-13	1,67	1,67
10e-14	1,81	1,87
10e-15	2,01	3,91
10e-16	2,06	**24,31**
10e-17	2,07	**228,31**
10e-18	2,07	**2268,3**

Appendix 5: Table with temperature values at different thicknesses

Thickness m	Production temperature (Finite fault)	Production temperature (Infinite Fault)
0.1	100,53	100.8
0.2	101.17	100.89
1	100.48	101.71
2	104.21	101.81
4	106.18	101.73
10	109.0	100.49

20	110.25	98.15
30	110.25	
40	109.87	
50	109.16	
60	108.22	85.05
70	107.19	
80	106.05	77.32
90	104.55	
100	102.79	69.06
110	101.02	
120	99.03	
130	98	
150	91.76	

Appendix 6: Table with impedance values at different thicknesses for finite and infinite fault with permeability of 10^{-14} m^2

Thickness (m)	MPa (Finite)	MPa (Infinite)
10	1,85	2,80
20	2,01	3,91
30	2,16	5,02
40	2,31	6,12
50	2,47	7,23
60	2,62	8,33
70	2,78	9,44
80	2,94	**10,54**
90	3,09	**11,65**
100	3,24	**12,75**
110	3,40	**13,86**
120	3,55	**14,69**
130	3,71	**16,07**
140	3,86	**17,17**
150	4,02	**18,27**